Penerbit
Akademia Baru

Advanced Research in Fluid
Mechanics and Thermal
Sciences

Predicting of Pool Boiling Heat Transfer From a Horizontal Heated Tube Using Two Fluids Multiphase Model

Open
Access

Mohammed Saad Kamel[1,2,*], Ferenc Lezsovits[1]

[1] Department of Energy Engineering, Faculty of Mechanical engineering, Budapest University of Technology and Economics, Hungary
[2] Department of Mechanical Techniques, Al-Nasiriya Technical Institute, Southern Technical University, Thi-Qar, Al-Nasiriya, Iraq

ARTICLE INFO	ABSTRACT
	This simulation aims to investigate numerically the pool boiling heat transfer from horizontal heated copper tube at atmospheric pressure. The Eulerian-Eulerian framework applied together with including Rensselaer Polytechnic Institute RPI boiling model to mimic the boiling process and predicting the heat and mass transfer inside the pool-boiling chamber. Efforts have been made in this simulation to correct the quenching heat flux part by modifying the bubble waiting time coefficient through adopting the trial and error procedure to correlate this coefficient to superheat temperature. The results of the boiling curve and the heat transfer coefficient of the present model are validated with experimental data from the literature and shown good agreement. Moreover, transient analysis of vapor volume fraction contours, vapor velocity vectors, and streamlines of water velocity at different superheat temperatures, as well as the time steps are presented and concisely discussed in this work.

1. Introduction

Boiling heat transfer is a significant heat transfer mode for industrial heat exchange systems due to the ability to remove a large quantity of heat in small superheat temperature. Boiling process and two-phase flow involved in many applications such as boiler tubes, evaporators, nuclear reactors, tubes bank or tubes bundles in heat exchangers [1-5]. To thoroughly understand the design of the heat exchange system, there is a necessity for understanding the critical factors of this phenomenon. Enhancement of boiling heat transfer coefficient and avoiding the critical heat flux CHF during the boiling process is one of the main tasks that investigators in the field of boiling are looking for to keep the systems safer and working with energy-saving [6-8]. Among all the regimes of pool boiling, the

---

* *Corresponding author.*
E-mail address: kamel@energia.bme.hu, kamel86@stu.edu.iq (Mohammed Saad Kamel)

nucleate pool-boiling regime considered as a most important and complex one due to complex nonlinear interactions of other related sub-phenomena related to bubble dynamics, heat transfer mechanism, and the topology of the heating surface and its thermal response [9]. Figure 1 illustrates a sketch of the mean affecting parameters on pool boiling heat transfer with immersion tubes.
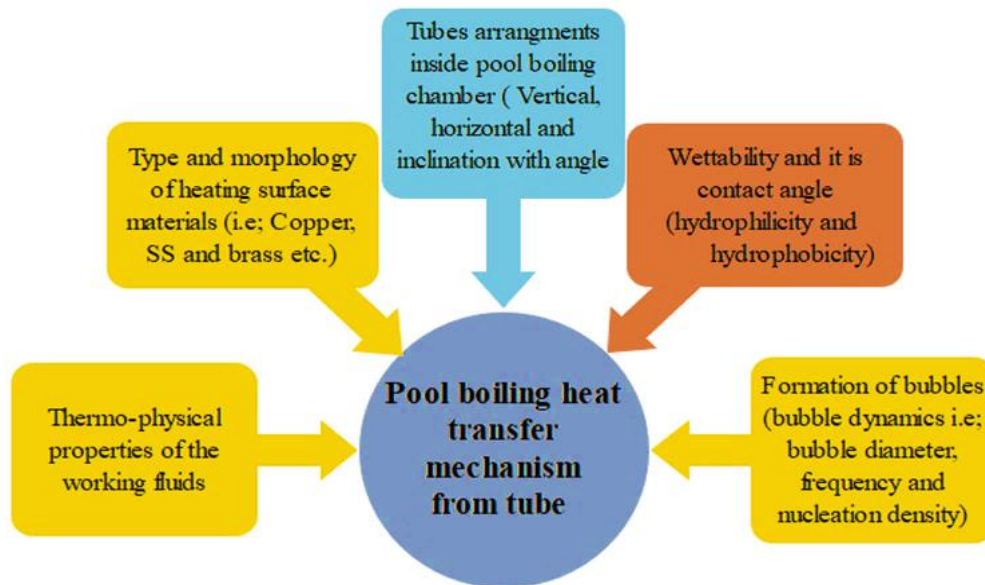
Fig. 1. Factors influenced the pool boiling on a heated tube

Many reported studies associated with pool boiling from the single tube or tubes bank introduced in literature utilizing experimental studies, and an empirical correlation was proposed to predict the heat transfer coefficient [10-15]. The accuracy of the proposed correlations is still challenging due to the presence of various parameters that are related to this mechanism. Water as a working fluid has extensive experimental studies for pool boiling heat transfer, and this perhaps due to the higher thermal properties compared to other liquids. Kang [13, 14] experimentally studied the pool boiling heat transfer of water from the tube with different position angels. He found that significant heat transfer mechanisms were considered to be liquid agitation induced by the sliding bubbles and the creation of large size bubbles column through bubble coalescence. Pool boiling on confined and unconfined tube columns was studied by Bartle and Walsh [16]. They developed a semi-empirical model from bubble plume images to evaluate bulk void fraction in an unconfined plume around a tube column. However, it was reported in the literature, there is still no robust model to predict the nucleate pool boiling accurately and this due to the strong interaction and significant parameters involved during this phenomenon. In the present work, we used the classical heat flux partitioning model under the boiling model rather than the interface tracking simulation method to introduce the boiling parameters which are involving the bubble dynamics behavior, and avoiding the computational costs for tracking bubbles from nucleation site distribution. Besides, this model could predict the heat flux by three mechanisms from the heated surface to bulk fluid in the proper way, which in turn, predicts the pool boiling heat transfer coefficient more accurately. The transient pool boiling of deionized water from the horizontal tube was numerically studied.

In this simulation, efforts have been made to predict the nucleate pool boiling heat transfer mechanism of water using the heat flux partitioning boiling model under a two-fluid Eulerian approach, which included and implemented closure correlations related to boiling parameters such as bubble departure diameter, nucleation site density as a build-in sub-models. Moreover, the bubble

waiting time coefficient in the quenching heat flux part was modified and correlated with superheating temperature to correct the quenching heat flux partition and enhance the obtained results. Finally, for the first time, contours of vapor volume fraction, vectors of vapor velocity and streamlines of water velocity from the single horizontal copper heated tube inside the pool chamber presented in this study. Results demonstrated that the heat transfer coefficient and boiling curve were in reasonable agreement with experimental work in literature.

2. Mathematical Formulation
2.1 Governing Equations

Two sets of conservation equations which govern the balance of mass, momentum, and energy of each phase are presented as follows [1, 17]:

Continuity equation:

$$\frac{\partial(\rho_k \alpha_k)}{\partial t} + \nabla.(\rho_k \alpha_k v_k) = \dot{m}_{kj} \tag{1}$$

Momentum equation:

$$\frac{\partial(\rho_k \alpha_k v_k)}{\partial t} + \nabla.(\rho_k \alpha_k v_k v_k) = \alpha_k \nabla P - \rho_k \alpha_k g + \nabla[\alpha_k \mu_k^e (\nabla v_k + (\nabla v_k)^T)] + (\dot{m}_{kj} v_k + \dot{m}_{jk} v_j) + S_{kj} \tag{2}$$

Energy equation:

$$\frac{\partial(\rho_k \alpha_k E_k)}{\partial t} + \nabla.(\rho_k \alpha_k v_k E_k) = \nabla[\alpha_k k_k^e (\nabla T_k)] + (\dot{m}_{kj} E_k + \dot{m}_{jk} E_j) + S_{kj} \tag{3}$$

where the subscripts of k and j are phase denotations (k, j= l for liquid phase and k, j= v for vapor phase. In these equations $\dot{m}_{kj}$ is the interfacial mass transfer of the water phase on the heating surface. In the bulk liquid, this quantity is equal to zero. This is because pool boiling begins at saturation temperature. $(\dot{m}_{kj} v_k + \dot{m}_{jk} v_j)$, In the momentum, the equation represents the momentum transfer due to liquid evaporation or vapor condensation. Also, $(\dot{m}_{kj} E_k + \dot{m}_{jk} E_j)$ in the energy equation stands for the energy transfer due to phase change.

2.2 The Heat Flux-Partitioning Model (RPI)

In the present study, the basic RPI model under the boiling model that be used by [18] was introduced to predict the boiling of water over a horizontal cylindrical tube. The total heat flux from the heated tube to the water partitioned into three main components, namely the convective, quenching, and evaporative heat flux as follows:

$$\acute{q}_{total} = \acute{q}_{conv} + \acute{q}_{quen} + \acute{q}_{evap} \tag{4}$$

The heated surface is subdivided into the area of a bubble created $A_{bubbles}$ and a portion, which is covered by the bulk liquid $(1 - A_{bubbles})$. The convective heat flux $\acute{q}_{conv}$ is expressed as following:

$$\acute{q}_{conv} = h_{single}(T_w - T_l)(1 - A_{bubbles}) \tag{5}$$

where h_{single} is the single-phase heat transfer coefficient, and $(T_w - T_l)$ is the difference between the surface and liquid temperatures. The second term is the quenching heat flux $\acute{q}_{quen}$, which models the cyclic averaged transient energy transfer associated with liquid filling on the heated surface vicinity after bubble detachment, and it is expressed as follows:

$$\acute{q}_{quen} = C_w \frac{2k_l}{\sqrt{\pi \lambda_l t}}(T_w - T_l) \tag{6}$$

where k_l, t, C_w and $\lambda_l = k_l / \rho_l Cp_l$ are the conductivity of the liquid, periodic time, the bubble waiting time coefficient, and the diffusivity of the fluid, respectively. The last term is the evaporative heat flux $\acute{q}_{evap}$, which is written as follows:

$$\acute{q}_{evap} = V_d N \rho_v h_{fv} f \tag{7}$$

where V_d is the volume of bubble based on bubble departure diameter, N is the nucleation site density, ρ_v and h_{fv} are the vapor density and latent heat of vaporization, respectively. Finally, f is the frequency of bubble departure.

2.3 Nucleate Boiling Parameters

All the equations mentioned above for heat flux partitioning model needs closure for boiling parameter that used for predicting the nucleate boiling process and those parameters described as following:

Nucleate site density: The nucleate site density usually correlated based on superheat wall temperature. The general formula is given:

$$N = C^n (T_s - T_{sat})^n \tag{8}$$

where $n = 1.805; C = 210$ are the empirical parameters that be used by Lemmert and Chawla [19], which is introduced in this study.

Bubble departure diameter: One of the essential nucleate boiling parameters is the bubble departure diameter D_w and several correlations used to introduce this parameter. In this study, the default bubble departure diameter for the RPI model was applied, and this correlation used by [20].

$$D_w = min\left(0.0014, 0.0006e^{(T_w - T_{sat})/45.0}\right) \tag{9}$$

Frequency of bubble: This parameter was reported to be decreased by increasing the bubble departure diameter. This fact is physically reasonable because the massive bubble needs a longer time to grow [21]. Cole correlation was used in this study to predict the frequency of bubble as follow:

$$f = \frac{1}{T} = \sqrt{\frac{4g(\rho_l - \rho_v)}{3\rho_l D_w}} \tag{10}$$

where ρ_l, ρ_v are the densities of liquid (water) and vapor, respectively. T, g are the bubble waiting time and the gravity acceleration force, respectively.

Area of influence: This area introduced based on bubble departure diameter and nucleation site density by [22] as follows:

$$A_{bubbles} = K \frac{N\pi D_w^2}{4} \tag{11}$$

This area has restricted to avoid the numerical instabilities due to unbound empirical correlations for nucleate site density. The final formula for this area becomes:

$$A_{bubbles} = \min(1, K \frac{N\pi D_w^2}{4}) \tag{12}$$

All formulation of interfacial forces for both phases (water) and (vapor) used in this simulation are modeled using correlations listed in Table 1.

3. Numerical Method

In this study, the physical geometry is a rectangular pool boiling chamber, and it was drawn in 2-Dimension according to the experiment pool boiling work of [29], as illustrated in Figure 2. The model geometry involving the heating surface is a horizontal copper tube with 10 mm, outside diameter, and the dimension of the pool boiling chamber was (150×100 mm). In this work, the nucleate boiling was carried out via transient state, and the transport equations were discretized by using finite volume method FVM and solved via commercial CFD code (Fluent 2019R2). To build the computational mesh, we used the meshing tool available in ANSYS. A grid independence test was done to check the grid sensitivity of the numerical results. Three grid elements were performed (10696, 15668, and 48906 elements) to verify the average vapor volume fraction around the tube at superheat temperature ($\Delta T_{sup} = 6$ K). The relative error for the average vapor volume fraction was less than 2.5%; hence, the second grid size selected to balance between the time and accuracy of the present results (see Table 2). The convective terms in all conservations equations approximated by a second-order upwind scheme and the gradient of the parameters calculated using the least-square cell-based method. All the closure correlations related to nucleate boiling of water that adopted in this work incorporated into the fluent solver as a build-in function.

Table 1
Models used in this simulation for the interfacial exchange of heat and mass transfer (phase interaction)

Physics	Model	Formulation
Virtual mass forces	Explicit source term	$\vec{F}_{VM} = C_{VM}\alpha_v\rho_l\left(\dfrac{d_l\vec{V}_l}{dt} + \dfrac{d_v\vec{V}_v}{dt}\right)$ where C_{VM} is the virtual mass coefficient and by default, it is equal to 0.5
Drag force	Schiller-Naumann [23]	$f = \dfrac{C_D Re}{24}$ $C_D = \begin{cases} \dfrac{24(1 + 0.15Re^{0.687})}{Re} & Re \leq 1000 \\ 0.44 & Re > 1000 \end{cases}$ $Re = \dfrac{\rho_l\|\vec{V}_v - \vec{V}_l\|}{\mu_l}$ $Re = \dfrac{\rho_{rv}\|\vec{V}_r - \vec{V}_v\|}{\mu_{rv}}$ where $\mu_{rv} = \alpha_v\mu_v + \alpha_r\mu_r$ is the mixture viscosity of vapor and mixture.
Lift force	Tomiyama [24]	$C_l = \begin{cases} min[0.288tanh(0.121Re_v), f(Eó_{modif})] & Eó_{modif} \leq 4 \\ f(Eó_{modif}) & 4 < Eó_{modif} \leq 10 \\ -0.27 & 10 < Eó_{modif} \end{cases}$ $f(Eó_{modif}) = 0.00105Eó_{modif}^3 - 0.0159Eó_{modif}^2 - 0.020Eó_{modif} + 0.474$ where Eo is modified Eotvos number and it is expressed as: $Eó_{modif} = \dfrac{g(\rho_v - \rho_l)d_h^2}{\sigma}$ $d_h = d_{b,d}(1 + 0.163Eo^{0.757})^{\frac{1}{3}}$ where d_h, $d_{b,d}$ are deformable bubbles and bubble diameters, respectivily. $Eo = \dfrac{g(\rho_v - \rho_l)d_{b.d}^2}{\sigma}$
Wall lubrication force	Antal *et al.,* [25]	$\vec{F}_{td,l} = -\vec{F}_{td,v} = C_{TD}\rho_l k_l \nabla\alpha_v$ C_{TD} is a user-modified constant, by default equal to 1
Turbulent interaction (mixture turbulence model)	Troshko-Hassan [26]	$F_{k_m} = C_{ke}\displaystyle\sum_{p=1}^{M} K_{pq}\left\|\vec{U}_l - \vec{U}_v\right\|^2$ $F_{\varepsilon_m} = C_{td}\dfrac{1}{\tau_p}F_{k_m}$ $C_{ke} = 0.75 \text{ and } C_{td} = 0.45$ $\tau_p = \dfrac{2C_{VM}d_p}{3C_D\|\vec{U}_l - \vec{U}_v\|}$
Heat Exchange Coefficient	Ranz-Marshall [27, 28]	$Nu_g = 2.0 + 0.6Pr_l^{0.333}Re_g^{0.5}$
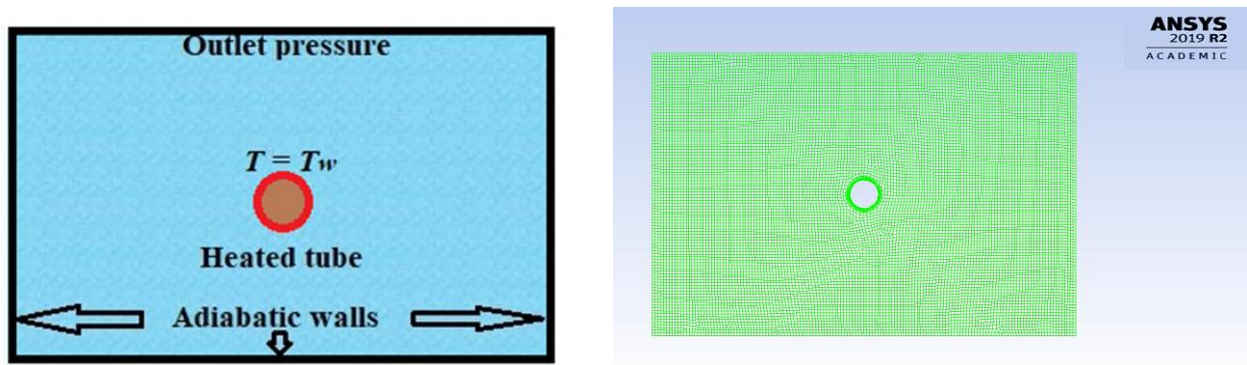
Fig. 2. Physical geometry for pool boiling chamber and grid structure

Table 2
Grid independence test for average vapor volume fraction at superheat temperature ($\Delta T_{sup} = 6$ K)

Parameter	Grid elements		Relative error %	Grid elements	Relative error %
	10696 elements	15668 elements		48906 elements	
Average vapor volume fraction [-]	0.292	0.299	2.3%	0.304	1.64%

The following assumptions were considered at this work:

i. The present simulation is transient and turbulence.
ii. The properties of water and vapor phases are assumed to be constant under the specified operating pressure and temperature, and all the properties were taken from the NIST chemistry webbook [30], as shown in Table 3.
iii. A time step size of (1 ms) selected for the present work. Moreover, the maximum iterations number per time step was set to be 100 after try and error procedure to assure that the solution is converged at each time step.

Table 3
Thermo-physical properties of water and vapor at saturation temperature (100 ℃) [30]

Property [Unit]	Water	Vapor
Saturation temperature [℃]	100	100
Density [kg/m^3]	958.35	0.598
Specific heat [$\frac{J}{kg}.K$]	4215	2080
Thermal conductivity [$\frac{W}{m}.℃$]	0.679	0.025
Viscosity [$Pa.s$]	2.8×10^{-4}	1.2269×10^{-5}
Latent heat of vaporization [kJ/kg]	2257.07	-
Surface tension [N/m]	0.0589	-
Prandtl number [-]	1.74	-

4. Boundary conditions

In the present simulation, the aforementioned governing equations are subjected to the following boundary conditions:

A constant temperature assumed to be at the heating surface of the horizontal tube.

$$T = T_w, \tag{13}$$

Heat flux is zero at the adiabatic walls of the boiling chamber.

$$q'' = -K_w \frac{\partial T}{\partial x} = 0, \tag{14}$$

At the top of the boiling chamber, the pressure is assumed to be atmospheric pressure.

$$P = P_{atm}, \tag{15}$$

5. Results and Discussion

The pool boiling heat transfer performance of water at atmospheric pressure from a horizontally heated copper tube was investigated in this simulation. This simulation aims to mimic with an accurate model the pool boiling heat transfer performance of water from a horizontal tube to investigate the contours, vectors, and streamlines of vapor and water phases inside the pool boiling chamber. Coming sub-sections describe the validation, results, and discussion of our simulation.

5.1 Model Validation

The results of the pool-boiling curve and pool boiling heat transfer coefficient PBHTC of water for a range of heat fluxes $29 - 87$ (kW/m^2) are presented in Figure 3 and 4. The present simulation results were validated with the experimental work of [29] and numerical work of [1], and the results of pool boiling curve and heat transfer coefficient are in good agreement with this experimental study, and this is because we used same geometry and boundary condition of [29]. The total heat flux was found to be close to experimental heat flux after taking in our consideration the uncertainties of the mentioned experimental work. The relative error found to be less than 3% for higher superheat temperature (10 K) in this simulation, which means that this simulation with a correction quenching heat flux part that represented by modifying the bubble waiting time coefficient model was quite acceptable to predict this phenomenon and enhanced the results of the numerical simulation. In this regard, efforts have been made to correct the quenching heat flux partition by modifying the bubble waiting time coefficient C_w in the quenching heat flux part (see, Eq. (6). see, Eq. (16) regarding the proposed correlation of bubble waiting time coefficient C_w as shown in Figure 5, fourth-degree polynomial function obtained with a coefficient of determination (R^2 = 1).

$$C_w = 0.0066\Delta T_{sup}^4 - 0.2174\Delta T_{sup}^3 + 2.5892\Delta T_{sup}^2 - 13.05\Delta T_{sup} - 23.664 \tag{16}$$

where C_w is the bubble waiting time coefficient [-], which introduced to correct the waiting time between the departures of sequential bubbles. The default value for this coefficient (equal to 1) in

Ansys fluent solver; however, we can modify this value as needed, but it can only be specified as a constant value. ΔT_{sup} is the superheat temperature [K]. The above correlation is valid for a range of heat flux $q^{.}$ $(29 < q^{.} < 87 \; kW/m^2)$ at atmospheric pressure.
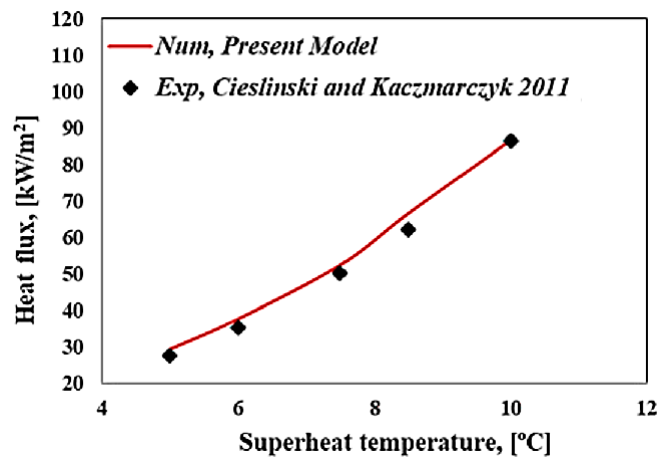
Fig. 3. Physical geometry for pool boiling chamber and grid structure
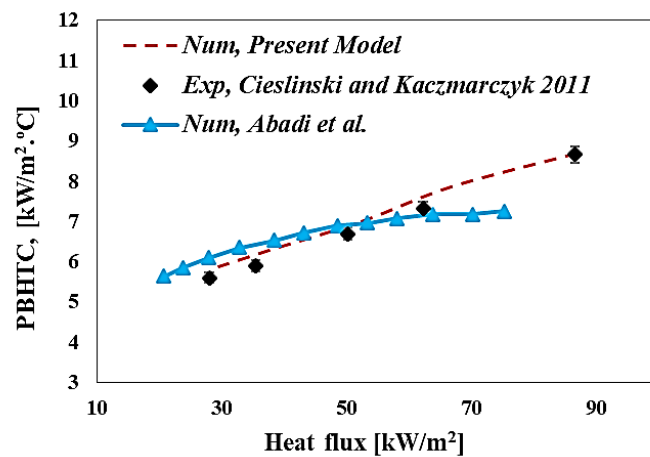
Fig. 4. Physical geometry for pool boiling chamber and grid structure
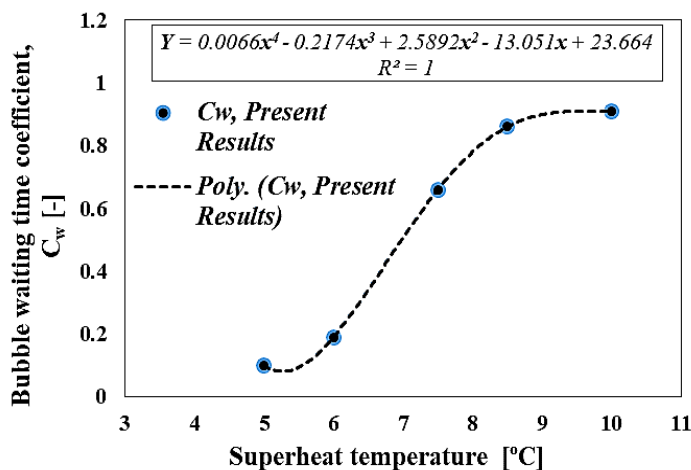
Fig. 5. Physical geometry for pool boiling chamber and grid structure

46

5.2 Contours of Vapor Volume Fraction

The formation of the vapor bubbles that represented by contours of vapor volume fraction concerning time steps and the different superheat temperatures were shown in Figure 6 and 7. At the time (t = 200 ms) and superheat (7.5 K), the bubbles begin to take shape on the circular horizontal heated tube and we can see that those gropes of bubbles start to sliding from bottom to sides of the tube then at a specific location they detached together and escapes to the top of the heated surface. As time increased to (t = 500 and 600 ms), bubbles started to travel the heated surface to the bulk fluid and became more abundant, and this is due to the buoyancy effects (vapor density less than water phase), which lifted the bubble to the top of the chamber. The height of this pool boiling was chosen according to experimental of [29] as mentioned in the previous section and due to the short distance between the heated tube and the surface of fluid the bubbles could not deform or shaped inside the bulk liquid to other forms then they were deformed in the top surface. Figure 7, Demonstrated the motion of bubbles at time (t = 600 ms) with various superheat temperature, as can be seen from the contours the vapor volume fraction increased with increasing the superheat temperatures and for superheat (10 K), the bubbles formed as a column and this due to the quantity of bubble that were created from the tube from various nucleation sites (increasing superheat temperature led to increasing the densities of the nucleation sites). The mechanism of sliding bubbles from the horizontal tube was reported in the literature [17, 31] through bubbles layer around the tube, and our simulation was physically matched this bubble layer, which is shown schematically in Figure 8. It can be concluded that the increase of superheat temperature significantly increases the nucleation site's density, which, in turn, led to increasing the bubbles number and the agitation of the fluids; hence, the heat transfer coefficient increase during this nucleate boiling regime. Some studies were reported this mechanism during the pool boiling heat transfer of liquid water from horizontal single and bank tubes [13, 14, 31].
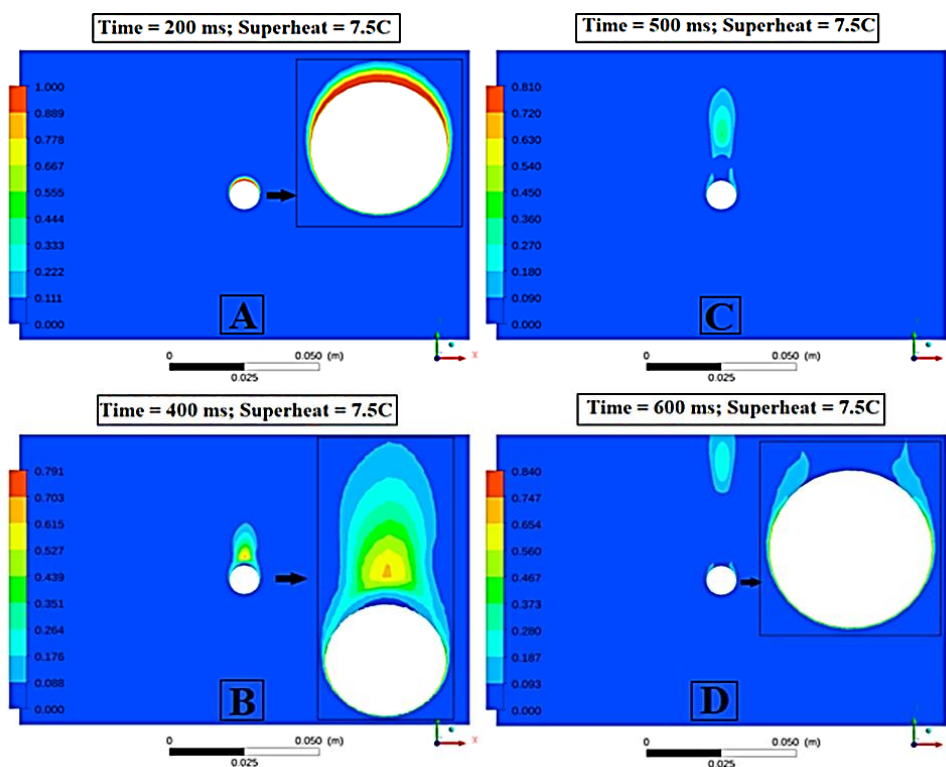
Fig. 6. Contours of vapor volume fraction with different time and superheat temperature (7.5 K); **A** (200 ms), **B** (400 ms), **C** (500 ms), and D (600 ms)
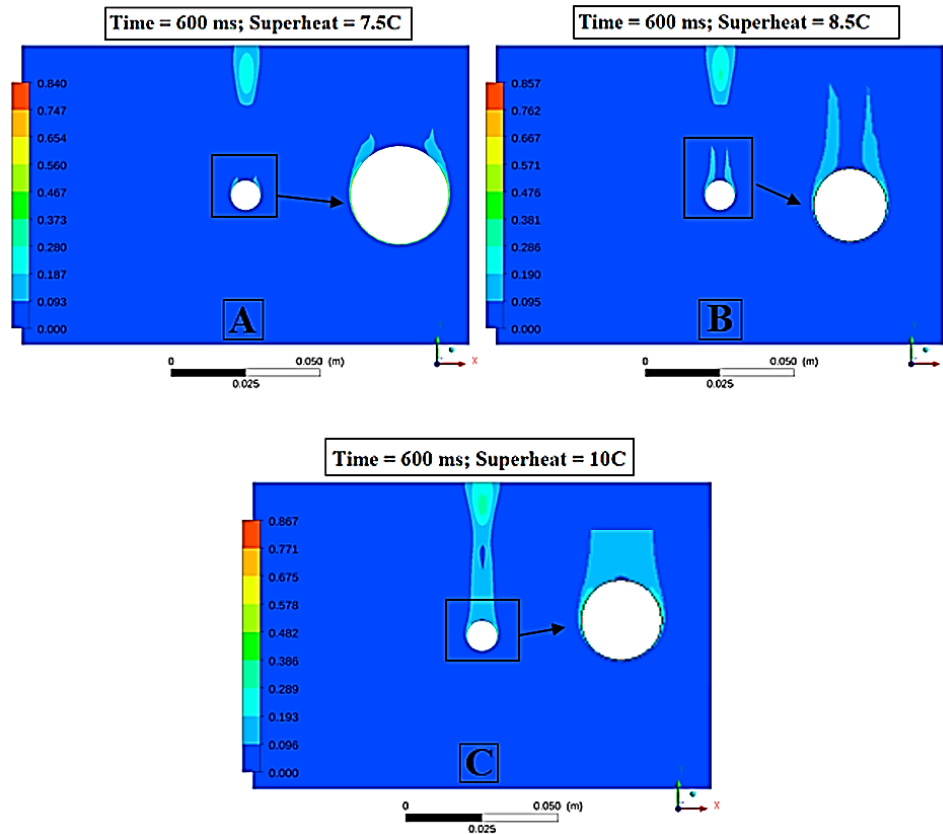
Fig. 7. Contours of vapor volume fraction at the time (600 ms) with different superheat temperatures; **A** (7.5 K), **B** (8.5 K), and **C** (10 K)
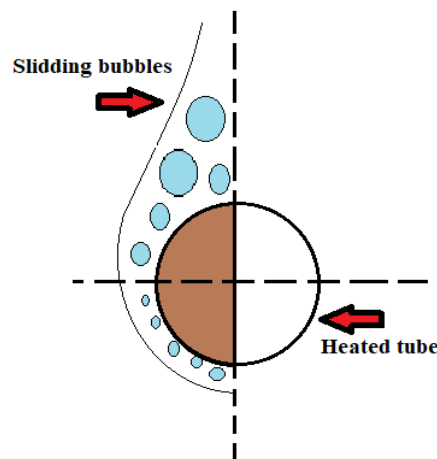
Fig. 8. Distribution of bubbles layer from horizontal tube immersion in a pool of liquid

5.3 Vapor Velocity Vectors

Figure 9 and 10 Depicts the vapor velocity vectors with different time steps and superheat temperatures. Figure 9, Shows the velocity of bubbles during the growth and sliding from the tube and this was introduced in terms of the vapor velocity vectors at different time steps and superheat (7.5 K). The velocity of bubbles at the bottom tube surface was high enough about (0.3 m/s) to slide on both sides of the circular tube to take away to the top of the boiling chamber. It can be seen that

from velocity distribution during bubbles formation at the heated surface start to increase as superheating temperature increase at the same time step as shown in Figure 10, and this due to the intensified bubbles columns from the sides tube. Line arrows demonstrated that vapor velocity increased with escaping time and increasing superheat temperature. It worth to mention that the velocity of bubbles at a circular heated tube starts to grow at sides tube then forms unify column of those bubbles which are vertically elapsed to the top bulk fluids surface. This was captured by visualizing study in literature [31], and hence, we can say that our model results match the experimental study by means physically during the pool boiling from the horizontal tube. Knowing the vapor velocity is very important during the condensation stage to understand the suitable cooling process.

5.4 Streamlines of Water Velocity

Figure 11 and 12 Presents the forward and downward streamlines of water velocity in the 2D pool boiling chamber with different time steps and superheat temperatures. The results have shown that the agitation of vapor (induced bubbles) from the tube towards the top side could move the water in the vertical direction and this stream could return downward and replace the water with fresh water (liquid circulation) and this mechanism may be increased as bubbles increased by increasing superheat temperature as shown in Figure 12, and this was reported by other studies in literature [32, 33]. This process introduces a reasonable explanation for the quenching heat flux part on the heated surface and water filling near departure bubbles, which called the transient quenching process, and this fact was mentioned in this model. The quenching model related to averaged transient energy transfer due to the liquid filling on the surface vicinity after the bubble departs with a period. On another hand, the streamlines of water velocity at constant superheat temperature (7.5 K) with different time steps were depicted in Figure 11. As can be seen from the streamlines the velocity of water at a time (200 ms), the vorticities are quite symmetrical at both sides of the chamber and this could be attributed to the tube position at the center of pool boiling chamber as well as the symmetrical dimension. The formation of bubbles from the tube towards the top of the chamber pushed the water upward, which results in these vorticities and replace the water with fresh water coming from the sides of the boiling chamber. This distribution could be significant for prediction the water velocities inside the pool-boiling chamber. Hence, accurate surface temperatures could be obtained by fixing the thermocouples in the right location during the experimental part; therefore, to get precise surface temperatures, measurement prediction of water velocities are essential in pool boiling experiments. Moreover, unlike other surface heating arrangements, the horizontal tube was the complicated arrangements due to the circulation of fluids, which makes the temperature measurements very sensitive around the tube direction.
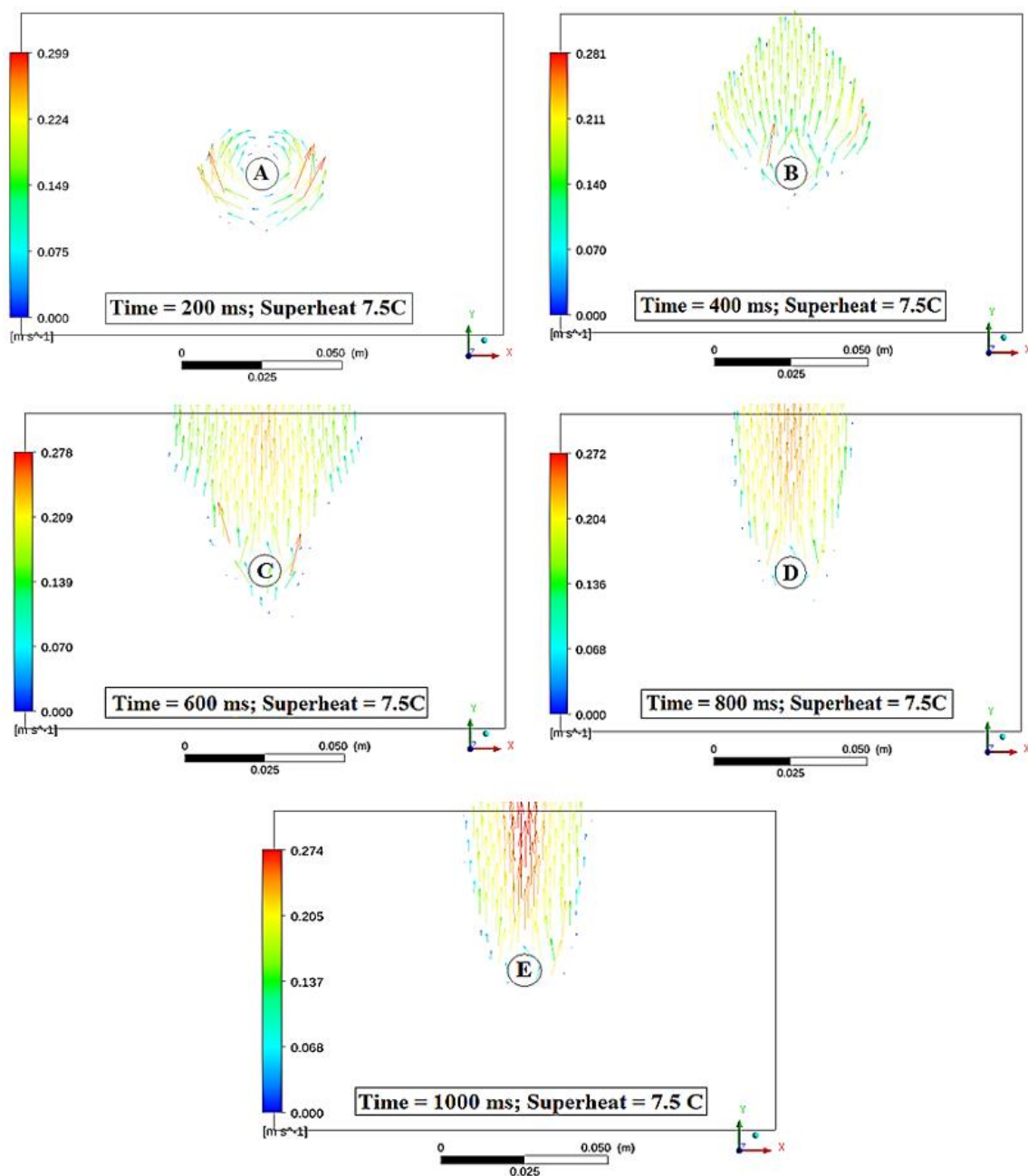
Fig. 9. Velocity vectors of vapor phase with different time and superheat temperature (7.5 K); **A** (200 ms), **B** (400 ms), **C** (600 ms), **D** (800 ms), and **E** (1000 ms)
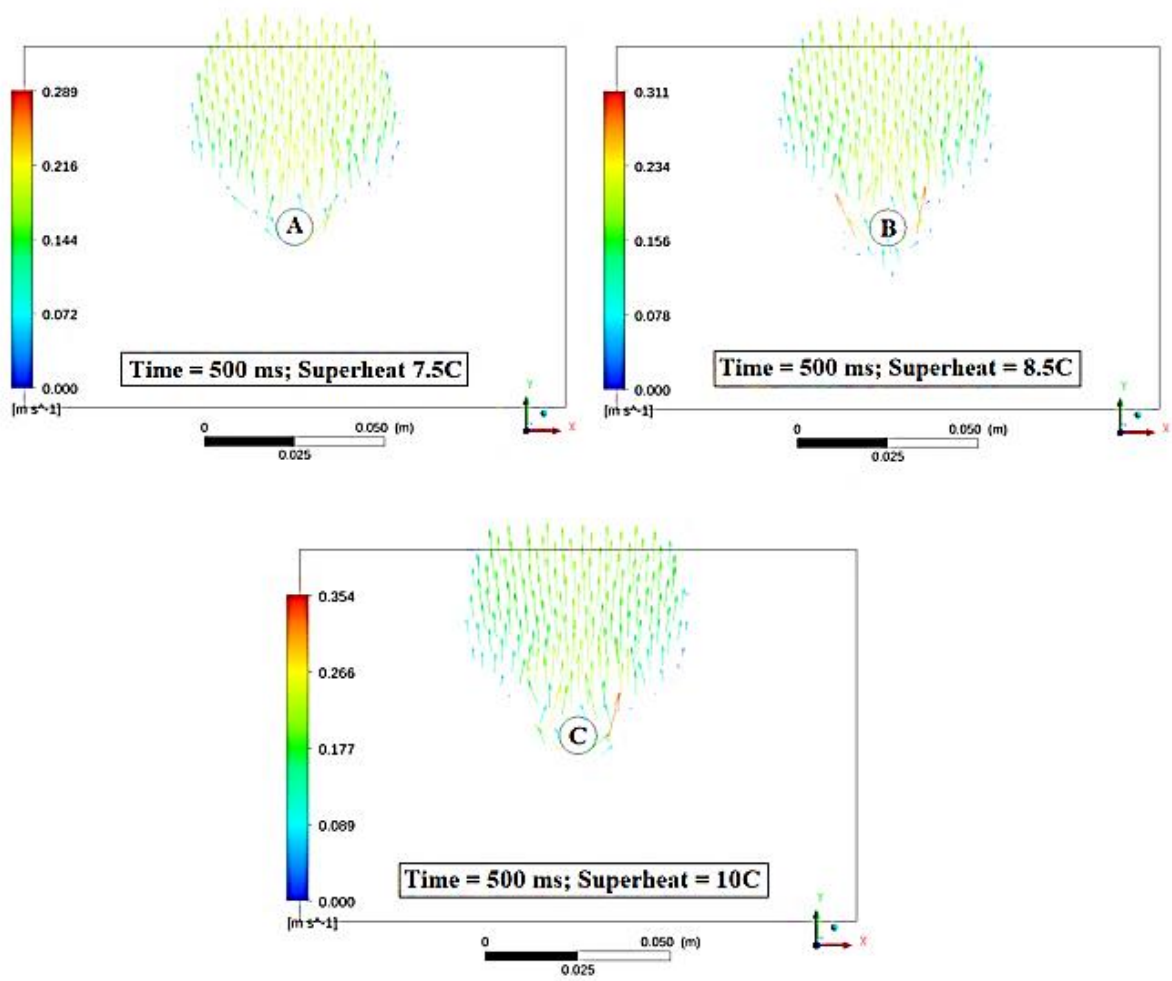
Fig. 10. Velocity vectors of vapor phase at the time (500 ms) with different superheat temperatures; **A** (7.5 K), **B** (8.5 K), and **C** (10 K)
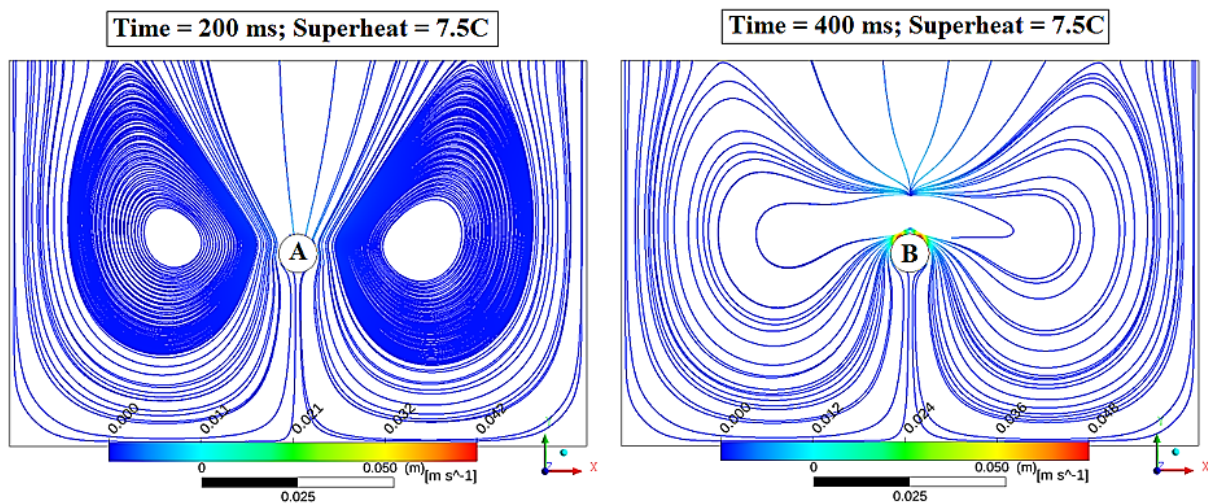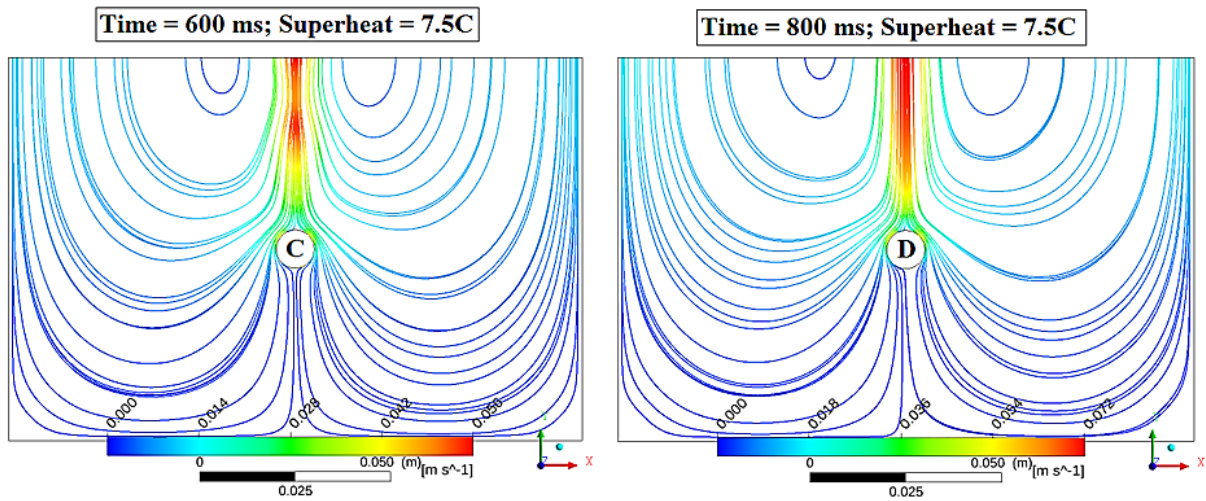
Fig. 11. Streamlines of water phase velocity at a different time and superheat temperature (7.5 K); **A** (200 ms), **B** (400 ms), **C** (600 ms), and **D** (800 ms)
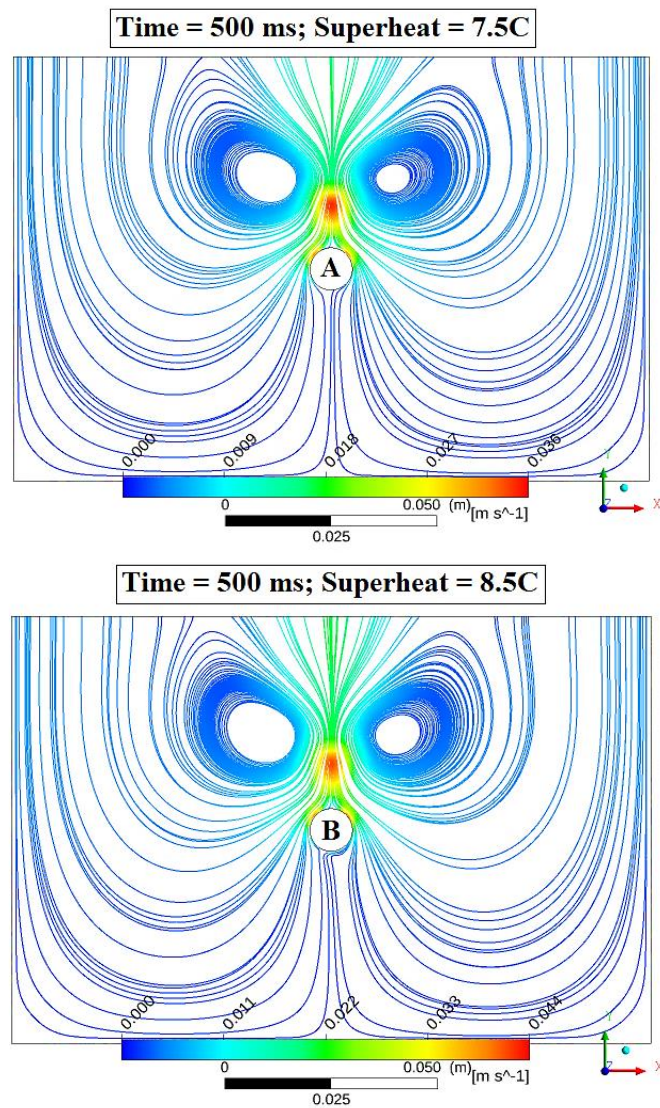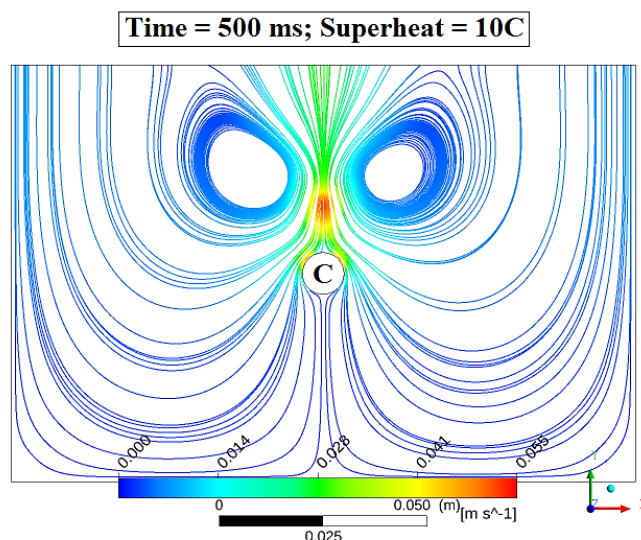
Fig. 12. Streamlines of water velocity at the time (500 ms) with different superheat temperatures; **A** (7.5 K), **B** (8.5 K), and **C** (10 K)

6. Conclusions

In the present simulation, the pool boiling heat transfer process of water using two fluids multiphase model was numerically investigated. The RPI model used to simulate this phenomenon, and we can conclude from this study the following points:

i. Nucleate pool boiling regime in the range of superheat temperatures ($5 - 12°C$) has been investigated using Heat flux partitioning model by adopting, and the results of the boiling curve and heat transfer coefficient validated with experimental work in literature and show good agreements.

ii. A new correlation for the bubble waiting time coefficient was proposed in this study by modified this coefficient via try and error procedure to correct the quenching heat flux partition, which is the component of the heat flux partitioning RPI model.

iii. Vapor volume fraction contours physically matched the visualization study of bubbles sliding from the horizontal tube in literature.

iv. Vapor velocity increase with increasing superheat temperature as a boundary condition in this study, and this was because the nucleation site density increase with increasing superheat temperature during the nucleate regime.

v. The streamlines of water velocity have been shown the circulation of water during the pool boiling process, and this could be a significant insight for predicting temperature measurements from a horizontal heated tube during the pool boiling phenomenon.

Conflict of interest

The authors declare that there is no conflict of interest.

References

[1] Abadi, SMA Noori Rahim, A. Ahmadpour, and Josua P. Meyer. "Numerical simulation of pool boiling on smooth, vertically aligned tandem tubes." *International Journal of Thermal Sciences* 132 (2018): 628-644.
https://doi.org/10.1016/j.ijthermalsci.2018.07.005

[2] Kamel, Mohammed Saad, Mohamed Sobhi Al-agha, Ferenc Lezsovits, and Omid Mahian. "Simulation of pool boiling of nanofluids by using Eulerian multiphase model." *Journal of Thermal Analysis and Calorimetry* (2019): 1-13.
https://doi.org/10.1007/s10973-019-09180-x

[3] Setyawan, A., Indarto and Deendarlianto. "Simplified correlation for liquid holdup in a horizontal two-phase gas-liquid annular flow." *Journal of Advanced Research in Fluid Mechanics and Thermal Sciences* 62, no. 1 (2019): 20-30.
http://www.akademiabaru.com/doc/ARFMTSV62_N1_P20_30.pdf

[4] Kamel, Mohammed Saad, Ferenc Lezsovits, and Ahmed Kadhim Hussein. "Experimental studies of flow boiling heat transfer by using nanofluids." *Journal of Thermal Analysis and Calorimetry* 138, no. 6 (2019): 4019-4043.
https://doi.org/10.1007/s10973-019-08333-2

[5] Kamel, Mohammed Saad, and Ferenc Lezsovits. "Boiling heat transfer of nanofluids: A review of recent studies." *Thermal Science* 23, no. 1 (2019): 109-124.
https://doi.org/10.2298/TSCI170419216K

[6] Sidik, N. A. C. and Alawi, O. A. "Computational investigations on heat transfer enhancement using nanorefrigerants." *Journal of Advanced Research Design* 1, no. 1 (2014): 35-41.
http://www.akademiabaru.com/doc/ARDV1_N1_P35_41.pdf

[7] Hegde, Ramakrishna N., Shrikantha S. Rao, and R. P. Reddy. "Investigations on heat transfer enhancement in pool boiling with water-CuO nano-fluids." *Journal of thermal science* 21, no. 2 (2012): 179-183.
https://doi.org/10.1007/s11630-012-0533-6

[8] Kamel, Mohammed Saad, Ferenc Lezsovits, Adnan M. Hussein, Omid Mahian, and Somchai Wongwises. "Latest developments in boiling critical heat flux using nanofluids: a concise review." *International Communications in Heat and Mass Transfer* 98 (2018): 59-66.
https://doi.org/10.1016/j.icheatmasstransfer.2018.08.009

[9] Dhir, Vijay K., Gopinath R. Warrier, and Eduardo Aktinol. "Numerical simulation of pool boiling: a review." *Journal of Heat Transfer* 135, no. 6 (2013).
https://doi.org/10.1115/1.4023576

[10] Das, Sarit K., Nandy Putra, and Wilfried Roetzel. "Pool boiling of nano-fluids on horizontal narrow tubes." *International Journal of Multiphase Flow* 29, no. 8 (2003): 1237-1247.
https://doi.org/10.1016/S0301-9322(03)00105-8

[11] Cieśliński, Janusz, and Tomasz Kaczmarczyk. "The effect of pressure on heat transfer during pool boiling of water-Al2O3 and water-Cu nanofluids on stainless steel smooth tube." *Chemical and Process Engineering* (2011): 321-332.
https://doi.org/10.2478/v10176-011-0026-2

[12] Trisaksri, Visinee, and Somchai Wongwises. "Nucleate pool boiling heat transfer of TiO2–R141b nanofluids." *International Journal of Heat and Mass Transfer* 52, no. 5-6 (2009): 1582-1588.
https://doi.org/10.1016/j.ijheatmasstransfer.2008.07.041

[13] Kang, Myeong-Gie. "Effects of elevation angle on pool boiling heat transfer of tandem tubes." *International Journal of Heat and Mass Transfer* 85 (2015): 918-923.
https://doi.org/10.1016/j.ijheatmasstransfer.2015.02.041

[14] Kang, Myeong-Gie. "Variation of local pool boiling heat transfer coefficient on 3-degree inclined tube surface." *Nuclear Engineering and Technology* 45, no. 7 (2013): 911-920.
https://doi.org/10.5516/NET.02.2013.001

[15] Sathyabhama, Alangar, and Ramakrishna N. Hegde. "Prediction of nucleate pool boiling heat transfer coefficient." *Thermal Science* 14, no. 2 (2010): 353-364.
https://doi.org/10.2298/TSCI1002353S

[16] Bartle, Roy S., and Edmond J. Walsh. "Pool boiling of horizontal mini-tubes in unconfined and confined columns." *International Journal of Heat and Mass Transfer* 145 (2019): 118733.
https://doi.org/10.1016/j.ijheatmasstransfer.2019.118733

[17] Salehi, H., and F. Hormozi. "Numerical study of silica-water based nanofluid nucleate pool boiling by two-phase Eulerian scheme." *Heat and Mass Transfer* 54, no. 3 (2018): 773-784.
https://doi.org/10.1007/s00231-017-2146-9

[18] Kurul, N., and Michael Z. Podowski. "Multidimensional effects in forced convection subcooled boiling." In *International Heat Transfer Conference Digital Library*. Begel House Inc., 1990.
https://doi.org/10.1615/IHTC9.40

[19] Lemmert, M., Chawla, L. M. "Influence of flow velocity on surface boiling heat transfer coefficient in Heat Transfer in Boiling." E. Hahne and U. Grigull, Eds., Academic Press and Hemisphere, New York, NY, USA, 1977.

[20] Tolubinsky, V. I., and D. M. Kostanchuk. "Vapour bubbles growth rate and heat transfer intensity at subcooled water boiling." In *International Heat Transfer Conference 4*, vol. 23. Begel House Inc., 1970.
https://doi.org/10.1615/IHTC4.250

[21] Cole, Robert. "A photographic study of pool boiling in the region of the critical heat flux." *AIChE Journal* 6, no. 4 (1960): 533-538.
https://doi.org/10.1002/aic.690060405

[22] Del Valle, Victor H., and D. B. R. Kenning. "Subcooled flow boiling at high heat flux." *International Journal of Heat and Mass Transfer* 28, no. 10 (1985): 1907-1920.
https://doi.org/10.1016/0017-9310(85)90213-3

[23] Schiller, Links. "A drag coefficient correlation." *Zeit. Ver. Deutsch. Ing.* 77 (1933): 318-320.

[24] Tomiyama, Akio. "Struggle with computational bubble dynamics." *Multiphase Science and Technology* 10, no. 4 (1998): 369-405.

[25] Antal, S. P., R. T. Lahey Jr, and J. E. Flaherty. "Analysis of phase distribution in fully developed laminar bubbly two-phase flow." *International Journal of Multiphase Flow* 17, no. 5 (1991): 635-652.
https://doi.org/10.1016/0301-9322(91)90029-3

[26] Troshko, A. A., and Y. A. Hassan. "A two-equation turbulence model of turbulent bubbly flows." *International Journal of Multiphase Flow* 27, no. 11 (2001): 1965-2000.
https://doi.org/10.1016/S0301-9322(01)00043-X

[27] Ranz, W. E., and W. R_ Marshall. "Evaporation from drops." *Chem. eng. prog* 48, no. 3 (1952): 141-146.

[28] Ranz, W. E., and W. R_ Marshall. "Evaporation from drops. Part II." *Chem. eng. prog* 48, no. 4 (1952): 173-180.

[29] Cieslinski, Janusz T., and Tomasz Z. Kaczmarczyk. "Pool boiling of water-Al 2 O 3 and water-Cu nanofluids on horizontal smooth tubes." *Nanoscale research letters* 6, no. 1 (2011): 220.
https://doi.org/10.1186/1556-276X-6-220

[30] Lemmon, E. W. "Thermophysical Properties of Fluid Systems, NIST chemistry WebBook, NIST standard reference database number 69." *http://webbook. nist. gov.* (2005).
https://doi.org/10.18434/T4D303

[31] Cornwell, Keith, and S. D. Houston. "Nucleate pool boiling on horizontal tubes: a convection-based correlation." *International journal of heat and mass transfer* 37 (1994): 303-309.
https://doi.org/10.1016/0017-9310(94)90031-0

[32] Aminfar, H., M. Mohammadpourfard, and M. Sahraro. "Numerical simulation of nucleate pool boiling on the horizontal surface for nano-fluid using wall heat flux partitioning method." *Computers & fluids* 66 (2012): 29-38.
https://doi.org/10.1016/j.compfluid.2012.05.019

[33] Qi, Cong, Yongliang Wan, Lin Liang, Zhonghao Rao, and Yimin Li. "Numerical and experimental investigation into the effects of nanoparticle mass fraction and bubble size on boiling heat transfer of TiO2–water nanofluid." *Journal of Heat Transfer* 138, no. 8 (2016).
https://doi.org/10.1115/1.4033353